ANALYTICAL SCIENCES MARCH 2020, VOL. 36

Microwave-assisted Synthesis of N,S-co-carbon Dots as Switch-on Fluorescent Sensor for Rapid and Sensitive Detection of Ascorbic Acid in Processed Fruit Juice

Sifan XU,* Shuqi YE, Yunhui XU,** Feifan LIU,** Yushun ZHOU,** Qian YANG,* Hailong PENG,*,** Hua XIONG,*† and Zhong ZHANG*,***†**

**State Key Laboratory of Food Science and Technology, Nanchang University, Nanchang 330047, China*
***School of Resources, Environmental, and Chemical Engineering, Nanchang University, Nanchang 330031, China*
****Shaanxi Engineering Laboratory for Food Green Processing and Safety Control, College of Food Engineering and Nutritional Science, Shaanxi Normal University, Xi'an 710119, China*

To achieve a rapid, sensitive, and economical method for the detection of ascorbic acid (AA) in the presence of Fe^{3+}, a nitrogen and sulfur co-doped carbon dots (N,S-co-CDs) based fluorescence sensing system was developed. In this work, N,S-co-CDs were successfully synthesized *via* a one-step microwave-assisted method within 2.5 min using ammonium citrate and L-cysteine as precursors. The fluorescence of N,S-co-CDs was quenched (off) by Fe^{3+} through a static-quenching mechanism. Subsequently, the fluorescence was recovered (on) after introducing AA into the quenched system, which was attributed to the reduction effect of AA for Fe^{3+}. Therefore, a switch-on sensor (N,S-co-CDs/Fe^{3+} system) was developed for AA detection. Under optimal conditions, the limit of detection (LOD) of 2.31 μmol/L for AA was obtained over a linear range from 0 to 150 μmol/L. Furthermore, the proposed sensing method was successfully applied to detect AA in processed fruit juice with satisfactory results. The most important is that the sensor derived from a microwave-assisted method has simple and eco-friendly synthesis processes, is rapid, and has high detection efficiency. Therefore, such a switch-on sensor may be a promising candidate sensor for AA detection in processed fruit samples.

Keywords Microwave-assisted synthesis, N,S-co-CDs, ascorbic acid, switch-on, processed fruit juice

(Received September 20, 2019; Accepted October 15, 2019; Advance Publication Released Online by J-STAGE October 25, 2019)

Introduction

Ascorbic acid (AA), commonly known as a soluble vitamin C, is an essential nutrient in many fruits and vegetables, which plays a vital role in biological metabolism and enzymatic reactions, such as immune cell development, connective tissue, tissue repair, and iron utilization redox signaling.[1,2] Additionally, AA is also associated with many chronic diseases, including gout, mucositis, infertility, skin disease, HIV/AIDS, and cancer.[2-5] However, AA is an exogenous substance and cannot be synthesized in the human body. Therefore, taking a daily supplement of AA *via* food diet is necessary for the human health. The main sources in the diet are fruits, vegetables and their products as well as dietary supplements containing AA. Unfortunately, AA in foods can be lost due to easy oxidation, particularly during thermal processing or storage. Hence, rapid detection of AA has great significance for accurate determination in processed foods. Until now, numerous techniques have been developed for AA detection, such as capillary electrophoresis,[6] chemiluminescence,[7] electrochemistry,[8] high performance liquid chromatography,[9,10] spectrophotometry,[11] chromatographic,[12] spectrofluorimetric,[13] and enzymology.[14] However, these techniques have different disadvantages of being time-consuming, high in cost, requiring complicated sample preparation, large infrastructure, and skilled personal. Therefore, more simple, rapid, effective, and sensitive methods for AA determination in food samples are still necessary.

Nowadays, all kinds of sensors, especially fluorescence sensors, have attracted more and more interest in the analytical field due to their high sensitivity and selectivity, easy operation, and low cost.[15] In the era of nanotechnology, fluorescent nanomaterials (*e.g.* quantum dots, metallic nanoclusters, luminescent nanoparticles) have emerged as an integrated research field because they offer superior optical properties, such as brighter fluorescence, wider selections of excitation and emission wavelengths, and higher photostability.[16] Among these fluorescent nanomaterials, quantum dots (QDs) have become more and more popular in fluorescent sensors for sample analyzing due to their highly luminous intensity, stability, and excellent spectral characteristics.[17,18] Till now, various QDs fluorescence sensors (*e.g.* CdTe,[19] Cu-ZnCdS,[20] MnO_2, MoS_2, and AuNCs) have been developed for highly sensitive and selective detection of AA in real samples.[21,22] However, these QDs exhibited various limitations, including complicated and expensive preparation processes, poor biocompatibility, and negative effect on food and the environment. Therefore,

† To whom correspondence should be addressed.
E-mail: huaxiong100@126.com (H. X.); zzhang@snnu.edu.cn (Z. Z.)

development of environmentally-friendly and safe QDs based fluorescent sensors for AA detection are urgently needed.

Compared with the above-mentioned QDs, carbon dots (CDs) exhibit various advantages such as low cost, simple synthesis route, better biocompatibility, lower cytotoxicity, high stability, no blinking fluorescence, and tunable excitation and emission spectra.[23] These advantages have made CDs widely applicable in biosensors,[24,25] optoelectronic devices,[26] drug delivery,[27,28] and light-emitting devices.[29,30] Unfortunately, as fluorescence sensors, CDs usually suffer from relatively low fluorescence quantum yields (FLQY) without surface doping with heteroatom. Previous reports have showed that heteroatom doping (*e.g.* N, S, B, Si and P) is a simple and efficient approach to improve fluorescence efficiency.[31,32] Among these doped CDs, N and S co-doped CDs are remarkably attractive with high FLQY.[33] And thus, N,S-co-CDs based fluorescence sensors have been widely applied in bioimaging, analytical, and pharmaceutical fields. Recently, N,S-co-CDs based fluorescence sensors, including N,S-co-CDs/Fe^{3+} and N,S-co-CDs/MnO_2 systems, have been applied to the detection of AA *via* "on-off-on" switchable model.[15,19]

In the N,S-co-CDs/Fe^{3+} system, the original fluorescence of N,S-co-CDs was firstly quenched by Fe^{3+} and then recovered by AA, which exhibited lots of merits, such as higher selectivity, nontoxicity, and high photo-induced electron transfer. However, the preparation method for N,S-co-CDs is extensively focused on the hydrothermal method, which is limited by time-consuming, rigorous experimental conditions, and difficulty of obtaining CDs powder directly. For the N,S-co-CDs/MnO_2 system, the disadvantages were hydrothermal method and involving heavy metal, which leads to toxicity of food and the environment. To overcome these limitations, the microwave-assisted method has been applied for the development of heteroatom doping CDs because it can offer intensive and homogeneous energy to reaction systems.[33-35] Numerous reports have shown that large-scale N,S-co-CDs powders with high FLQY can be directly obtained *via* microwave-assisted method.[36,37] However, to the best of our knowledge, application of N,S-co-CDs *via* microwave-assisted method as a fluorescence sensor has been rarely reported.

Herein, in this study, large-scale N,S-co-CDs powders with high FLQY were directly prepared *via* one-step microwave-assisted method. The FL of N,S-co-CDs can be quenched by Fe^{3+} (off) and then recovered (on) after introducing AA. Thus, a switch-on fluorescence sensor was developed and its properties were investigated for explaining the possible detection mechanism. Meanwhile, the detection conditions were optimized and corresponding analytical performances were researched systematically. The developed switch-on sensor possessed high sensitivity and excellent selectivity toward AA. Furthermore, the switch-on sensor was successfully applied for AA detection in processed fruit juice. Therefore, the developed switch-on fluorescence sensor may be a simple, rapid and selective detection method for AA detection in processed fruit samples.

Materials and Methods

Reagents and chemicals

Ammonium citrate (AC), ascorbic acid (AA), acetic acid, sodium acetate, oxalic acid, citric acid, and malic acid were purchased from XiLong Chemical Co. Ltd. (Shantou, Guangdong, China). L-(+)-Tartaric acid (TA) was purchased from Tianjin DaMao Chemical Factory (Tianjin, China). L-Cysteine (Cys) was obtained from Beijing Solabio Technology Co., Ltd. (Beijing, China). Glutathione (GSH) and 1,10-phenanthroline were purchased from Aladdin (Shanghai, China). All other reagents were of analytical grade and used without further purification. Ultrapure water used throughout the work was produced by a Milli-Q Ultrapure water system (Millipore, Bedford, USA). The fruit samples were obtained from a local supermarket (Nanchang, Jiangxi).

Characterization

Morphology of N,S-co-CDs was performed using transmission electron microscope (TEM, JEOL, JEM-2010HR, Japan). The Fourier transform infrared (FT-IR) spectra were recorded by using the FT-IR spectrophotometer (Nicolet 5700, Thermo Electron Corporation, MA,USA). The X-ray diffractometer (XRD) patterns were recorded using XRD analyzer (D8-FOCUS, Bruker, Karlsruhe, Germany). Zeta potential was measured using a Malvern Zeta/size Nano-ZS90 (ZEN3590, UK). UV-vis spectra were collected on a Model Scinco UV TU-1900 (China). Fluorescence spectra were recorded at room temperature using a F-7000 fluorescence spectrophotometer equipped with a xenon flash lamp (Japan). The slit widths of excitation and emission were both 5 nm.

Synthesis of N,S-co-CDs

N,S-co-CDs were synthesized by one-pot microwave-assisted method according to a previous report with certain modifications.[38] Briefly, AC (2 g, 9.6 mmol) and Cys (1 g, 8.3 mmol) were dissolved in 10 mL ultrapure water. The mixture was sonicated for 3 min to form a transparent solution. The solution was irradiated in a domestic microwave oven (700 W) for 2.5 min. After that, water was evaporated and brownish powders were obtained directly. The powders were dissolved into ultrapure water, and filtered through a 0.22 μm filter membrane to remove any insoluble particles. The filtrate was collected and further diluted to 100 mL with ultrapure water and stored at 4°C for further use.

Quantum yield measurements

The quantum yields of N,S-co-CDs were determined by using quinine sulfate as the fluorescence standard and were calculated according to the following equation:

$$Y_u = Y_{st} \times (I_u/I_{st}) \times (A_{st}/A_u) \times (n_u^2/n_{st}^2) \quad (1)$$

where Y is the quantum yield, I is the measured integrated emission intensity, n is the refractive index, and A is the extinction. The subscript "st" refers to the standard and "u" refers to the sample with unknown QY.

Fluorescence sensing of AA

The process of AA sensing was performed as follows. Firstly, 100 μL of N,S-co-CDs solution and a known amount of Fe^{3+} were successively added into 1 mL acetate buffer (pH 6.0, 0.01 M) to incubate at room temperature for 15 min. Thereafter, various concentrations of AA standard solutions were added into the mixtures (N,S-co-CDs/Fe^{3+}) and then were diluted to 4 mL. Fe^{3+} with a final concentration was 0.5 mmol/L. After incubating at room temperature for 15 min, all FL spectra were measured at excitation wavelength of 350 nm and emission wavelength of 425 nm. All samples for fluorescence measurements were performed in triplicate.

Analysis of processed fruit juice

All of the samples were purchased from a local supermarket

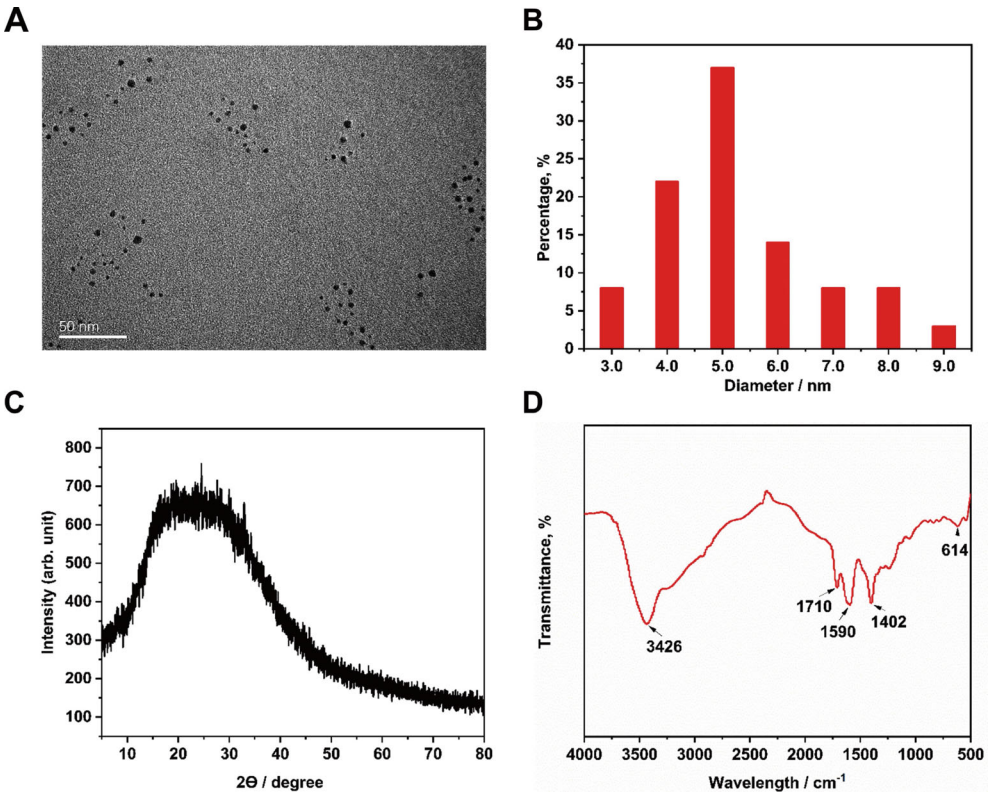

Fig. 1 Characterization of N,S-co-CDs (A) TEM images, (B) the particle size distribution, (C) XRD spectrum, (D) FT-IR spectrum.

(Nanchang, China). Fresh fruits (kiwi, tomato, citrus reticulata, mango, and apple) samples were prepared according to the procedure described in a previous paper.[19] First, all of the samples were washed with ultrapure water and dried naturally in air at room temperature. These fruits were then accurately weighed and homogenized using a commercial blender. After centrifugation at 4°C (4000 rpm) for 15 min, the supernatant was filtered through a 0.45 µm pore size filter membrane and then diluted to an appropriate concentration in the detection range with ultrapure water. The final juices of kiwi, mango, tomato, citrus reticulata, and apple were diluted to 50, 30, 20, 15, and 4 times, respectively. Detection procedures of AA in processed fruit juice were the same as in the standard samples. The analysis data ($n = 3$) were collected and subjected to statistical analyses.

Results and Discussion

Characterization of N,S-co-CDs

N,S-co-CDs were prepared by the microwave-assisted method using AC as C and N source, and Cys as N and S source, respectively. The synthesized N,S-co-CDs have good fluorescent ability under optimized conditions of the mass ratio of AC/Cys (2/1). Meanwhile, the Y_u of N,S-co-CDs powders was about 51.50% within 2.5 min. These results showed that the microwave-assisted method exhibited simple, rapid, higher yield, and eco-friendly advantages compared with traditional approaches for CDs preparation due to its intensive, efficient and homogeneous energy distribution.

For development of a favorable switch-on fluorescent sensor, the characterizations of N,S-co-CDs, including morphology, element composition, and optical properties, were investigated in detail. The morphology of N,S-co-CDs were observed using TEM and the results are shown in Fig. 1A, suggesting that the N,S-co-CDs exhibited a spherical shape with uniform dispersion. Meanwhile, the size distribution of N,S-co-CDs ranged from 2.0 to 8.8 nm and the average diameter was 4.8 nm (Fig. 1B). The XRD pattern was used to confirm the N,S-co-CDs structure (Fig. 1C), showing that one big peak at about 24.0° appeared, which was assigned to the highly disordered C species with a high degree C (002) plane for a partially graphitized structure, confirming the amorphous carbon phase of N,S-co-CDs.[37]

The element compositions of N,S-co-CDs were investigated using FT-IR and EDS. The FT-IR result was shown in Fig. 1D, it can be seen that the C–O stretching vibration at 3426 cm^{-1} appeared, which showed –OH groups on the N,S-co-CDs surface. The adsorption peak at 1710 cm^{-1} was attributed to the stretching vibration of the C=O group. The peaks at 1590 and 1402 cm^{-1} were attributed to C=C and C–N groups. Meanwhile, the peaks at 614 cm^{-1} were due to the stretching vibration of C-N/C-S groups. The EDS result of N,S-co-CDs is shown in Fig. S1 (Supporting Information), and it can be seen that the element compositions were C, N, O, and S with corresponding content value of 3.76, 10.74, 67.22, and 18.28%, respectively. The FT-IR and EDS results indicated that N,S-co-CDs were successfully doped with N and S elements. The zeta-potential of N,S-co-CDs was about –8.28 mV (Fig. S2, SI), which was owing to abundant –COOH and –OH groups on the N,S-co-CDs surface. However, the zeta-potential decreased to –15.70 mV after adding Fe^{3+} into N,S-co-CDs solutions, suggesting that Fe^{3+} can be interacted with the carboxyl and amine groups of N,S-co-CDs.[38,39]

The optical properties of N,S-co-CDs were investigated using

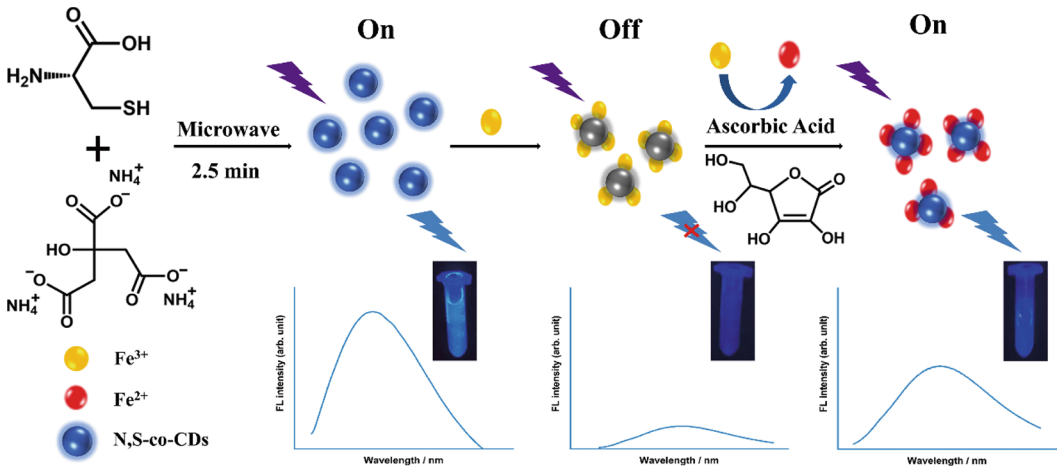

Scheme 1 Schematic illustration of mechanism of the fluorescence turn-on detection of AA based on N,S-co-CDs.

UV and fluorescence spectrum (Fig. S3A, SI). It can be seen that two distinct absorption peaks appeared at 248 and 345 nm. The peak at 248 nm was due to the π-π* transition of the C=O band and no obvious fluorescence signal in this peak.[33] Fortunately, the 345 nm absorption was attributed to n-π* transition of C=O or C–OH, which can form strong fluorescence emission because of the recombination of localized surface states and excited-state energy.[40] From Fig. S3A (SI) we can see that the excitation and emission N,S-co-CDs wavelength was about 350 and 425 nm, respectively, suggesting that such N,S-co-CDs has an excellent potential application in the analytical field. Meanwhile, a bright blue-fluorescence appeared under UV light irradiation (365 nm) for N,S-co-CDs with excellent dispersion in water. To further study the optical properties of N,S-co-CDs, the emission spectrum were measured at different excitation wavelengths ranging from 300 to 380 nm, and the results are shown in Fig. S3B (SI). These results showed that the synthesized N,S-co-CDs using microwave-assisted method exhibited excitation-independent properties without further purification. To investigate the stability during the storage period, N,S-co-CDs solution was illuminated sustainably under UV light (350 nm) in 60 min and the fluorescence was detected every 2 days to evaluate long-term storage stability under ambient conditions. As shown in Fig. S4 (SI), there was no obvious changes in fluorescence after 60 min of continuous illumination at 350 nm and 30 days at ambient conditions, indicating that the developed N,S-co-CDs exhibited excellent stability.

Design principle and mechanism of sensor for AA

Scheme 1 schematically suggests the preparation processes for a switch-on fluorescent sensor for AA sensing. The microwave-assisted method can effectively offer both rapid and uniform heating of the reaction medium, which can shorten the reaction time and greatly improve the product yield and purity. Therefore, the microwave-assisted method was applied to synthesize N,S-co-CDs using ammonium citrate and L-cysteine as precursors within 2.5 min in this investigation. N,S-co-CDs exhibited stronger fluorescent capability with carboxyl and amine groups on its surface, which can interact with Fe^{3+} and then quench the fluorescent of N,S-co-CDs. Additionally, AA can reduce Fe^{3+} to Fe^{2+}, which showed much lower ability to chelate N,S-co-CDs. Therefore, the fluorescence was partly recovered when AA was introduced into the N,S-co-CDs/Fe^{3+} system. The detailed sensor mechanisms were investigated as follows.

UV-vis absorption spectrum of N,S-co-CDs, N,S-co-CDs/Fe^{3+}, and Fe^{3+} were measured and the results are shown in Fig. 2A, which indicated that UV-vis spectra of N,S-co-CDs were greatly changed with Fe^{3+} addition compared to that of N,S-co-CDs or Fe^{3+}. It is obvious that the complex chelates *via* Fe^{3+} and the carboxyl and amine groups on N,S-co-CDs surface were formed. A previous report showed that the photo-induced electron transfer (PET) was the quenching mechanism for the N,S-co-CDs/Fe^{3+} system because Fe^{3+} is a kind of paramagnetic transition metal ions with half-filled 3d orbits.[15] However, it is noted that there is no spectral overlap between UV absorption spectrum of Fe^{3+} and the fluorescence emission spectrum of N,S-co-CDs (Fig. 2B) in our study, which indicated that fluorescence resonance energy transfer (FRET) was not the possible quenching mechanism for the N,S-co-CDs. Fluorescence quenching requires a molecular contact between the fluorophore and the quencher. The contact can be the result of diffusive encounter and complex formation, which corresponds to dynamic and static quenching, respectively. Generally, the dynamic and static quenching can be described by the Stern–Volmer equation as follows:[41]

$$F_0/F = 1 + K_S[Q] = 1 + K_D[Q] \quad (2)$$

Where K_s and K_D are the Stern–Volmer constants for the static and dynamic quenching process, respectively, Q is the quencher concentration; F_0 and F are the fluorescence in the absence and presence of Fe^{3+}, respectively. According to the Stern–Volmer equation, the plot of Fe^{3+} ions in the range of 0 – 300 μM exhibited good linearity in the N,S-co-CDs/Fe^{3+} system (Figs. 2C and 2D). The K_s value (2.36×10^3 L/mol) was obtained after fitting of the quenching data, which was far greater than the maximum diffusion-rate constant of 100 L/mol, suggesting that the fluorescence quenching mechanism of the N,S-co-CDs/Fe^{3+} system was initiated by the static-quenching effect, which was the result of the formation of a nonfluorescent ground-state complex between the quencher (Fe^{3+}) and fluorophore (N,S-co-CDs), and the generated complex absorbed light could immediately return to the ground-state without any photon emission.[42]

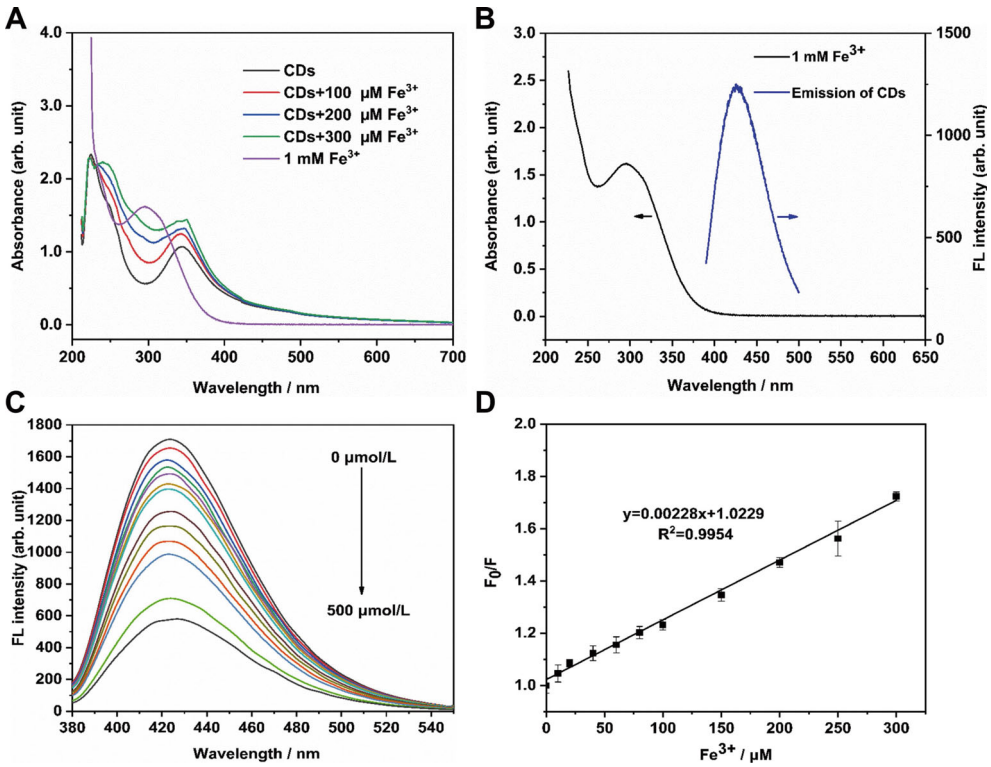

Fig. 2 (A) UV-vis absorption spectra of N,S-co-CDs, N,S-co-CDs/Fe^{3+} and Fe^{3+}. (B) UV-vis absorption spectrum of Fe^{3+} (black line) and fluorescence emission spectrum of N,S-co-CDs (blue line). (C) Fluorescence emission spectra of the N,S-co-CDs in the presence of different Fe^{3+} concentrations. (D) The linear relation of F_0/F *versus* concentration of Fe^{3+} over the range of 0 – 300 μM.

As shown in Fig. S5 (SI), the fluorescence was gradually recovered with increasing AA concentrations in the N,S-co-CDs/Fe^{3+} system. However, the fluorescence has not obviously changed when single AA was added into the N,S-co-CDs solution in the absence of Fe^{3+}, indicating that AA cannot interact with N,S-co-CDs and then did not affect its emission ability. It is obvious that the recovery mechanism of fluorescence was mostly due to the reaction between Fe^{3+} and AA. As shown in Fig. S6 (SI), the mixtures (N,S-co-CDs/Fe^{3+} + AA) in the presence of 1,10-phenanthroline presented an obvious absorption at 510 nm compared to the N,S-co-CDs/Fe^{3+} system, which can be resulted by the orange-red complex of Fe^{2+} and 1,10-phenanthroline. The results indicated that Fe^{3+} was reduced to Fe^{2+} by AA in the N,S-co-CDs/Fe^{3+} system, and Fe^{2+} exhibited much lower ability to chelate N,S-co-CDs and then the fluorescence can be partly restored.

Based on the above-mentioned phenomenon, N,S-co-CDs were synthesized *via* microwave-assisted method using ammonium and L-cysteine as precursors. And then, a simple and cost-effective switch-on sensor (N,S-co-CDs/Fe^{3+} system) was developed for selective AA detection.

Optimization of AA detection conditions

To obtain the best sensing response of the switch-on sensor for AA, the potential effects of detection parameters, including detection system pH, Fe^{3+} concentration, and quenching and recovery incubation time, were all investigated in detail.

As the pH value of the sensing system is critical, the effect of pH was in the range of 3 – 10. As shown in Fig. 3A, the FL of N,S-co-CDs quickly increased in the pH range of 3 – 6 and insignificantly changed in pH 6 – 10. However, the fluorescence significantly decreased when Fe^{3+} was added into N,S-co-CDs solution at pH 6. Additionally, Fe^{3+} exhibited good stability and had stronger interaction capability with N,S-co-CDs at pH 5 – 6. Meanwhile, AA was easily oxidized when the pH value was higher than 7. Thus, pH 6.0 was employed in this sensing system for subsequent experiments.

In the N,S-co-CDs/Fe^{3+} system, the Fe^{3+} concentration plays a vital role in the sensor sensitivity because excessive or insufficient Fe^{3+} can lead to low quenching and recovery efficiency. Therefore, the effect of Fe^{3+} concentration was investigated and the results are shown in Fig. 3B. The results suggest that the quenching efficiency dramatically increased with Fe^{3+} concentration from 0.3 to 1.5 mM, but fluorescence recovery efficiency slowly increased and then declined dramatically, getting higher at 0.4 and 0.5 mM. Based on the above factors, Fe^{3+} concentration of 0.5 mM was applied in the further experiments.

To get an ideal response time for AA using the switchable sensor, the quenching and recovery time was investigated and the results are shown in Figs. 3C and 3D. It was clearly shown that the fluorescence of N,S-co-CDs gradually decreased after adding Fe^{3+} (0.5 mM) with incubation time from 0 to 15 min and leveled off to stable constant values. However, the fluorescence of the N,S-co-CDs/Fe^{3+} system can be recovered quickly to stable within 15 min. Accordingly, 15 min was adopted as the quenching and recovery incubation time.

Switch-on sensing of AA

For sensing AA, different concentrations of AA (0 – 500 μmol/L)

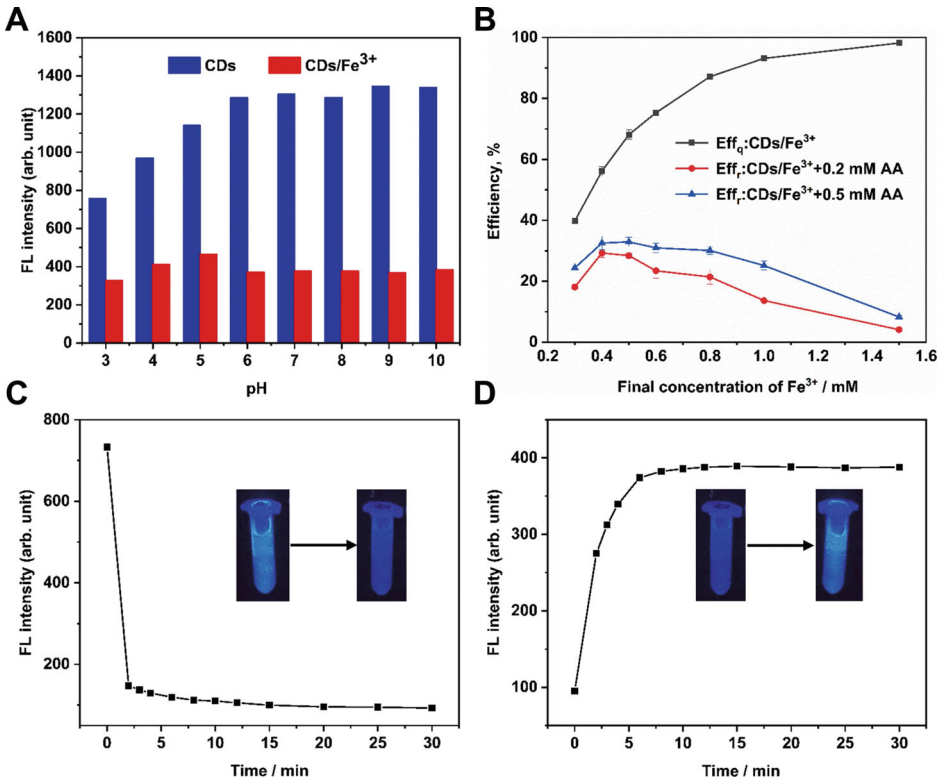

Fig. 3 (A) FL intensity of N,S-co-CDs and N,S-co-CDs/Fe^{3+} at different pH solution. (B) Effects of Fe^{3+} concentration to Eff_q and Eff_r. $Eff_q(\%) = (F_0 - F)/F_0$, $Eff_r(\%) = (F_r - F)/(F_0 - F)$, where F and F_0 represented the FL intensity of N,S-co-CDs in the presence and absence of Fe^{3+}; F_r is recovered fluorescence intensity of N,S-co-CDs after adding AA. Relationships between fluorescence intensity and (C) the incubation time of quenching and (D) the time needed for restoration, respectively.

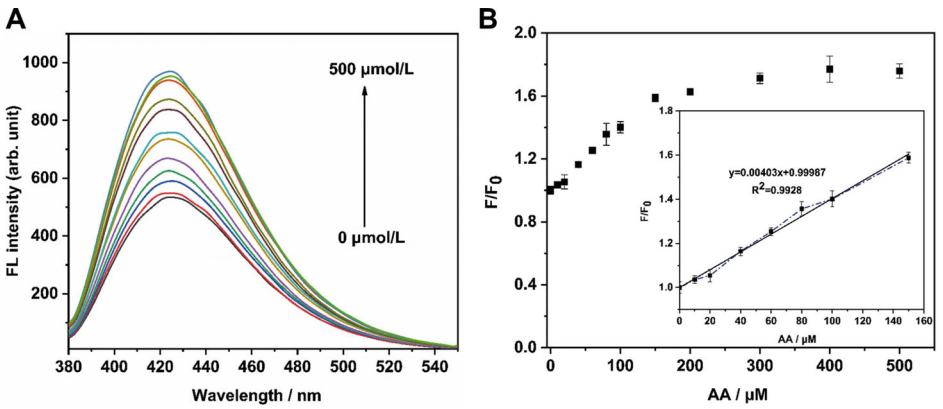

Fig. 4 (A) Fluorescence emission spectra of the N,S-co-CDs in the presence of 0.5 mmol/L Fe^{3+} and AA at different concentrations. (B) Plot of the fluorescence recovery factor (F/F_0) *versus* concentration of AA (inset: a linear region).

were added into the switch-on sensor (N,S-co-CDs/Fe^{3+} system) and then the fluorescence was measured under optimal conditions. As shown in Fig. 4, the fluorescence of the switch-on sensor was gradually restored with increasing AA concentration from 0 to 150 μmol/L. The plot of fluorescence restoration factor F/F_0 *versus* AA concentrations was obtained and exhibited a good linear relationship in the range of 0 – 150 μmol/L. The regression equation was $F/F_0 = 0.00403C + 0.999$, and a high correlation coefficient ($R^2 = 0.993$) was obtained. Meanwhile, the corresponding LOD (2.31 μmol/L) was calculated based on a signal-to-noise ratio of 3. The comparison of reported fluorescent sensors for AA detection is shown in Table S1 (SI), showing that most fluorescent sensors were developed using hydrothermal and pyrolysis methods involving heavy metal ion, which leads to the disadvantages of requiring much time, higher cost, lower-scale production, and pollution to the environment and food. In spite of the fact that the acceptable LOD (2.31 μmol/L) of this work was a little higher than that of these sensors derived from the hydrothermal and pyrolysis methods (Table S1), it is noted that our switch-on

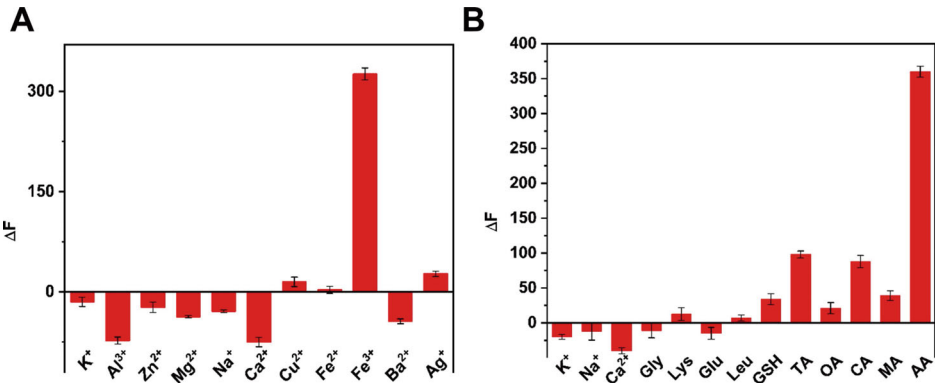

Fig. 5 (A) Selectivity of N,S-co-CDs platform for Fe^{3+} detection. The concentrations of metal ions are 125 μmol/L. (B) Selectivity of the N,S-co-CDs/Fe^{3+} platform toward ascorbic acid (100 μmol L^{-1}), the concentration of the ions are 10-fold concentration of AA and except interfering species are 5-fold concentration of AA. Error bars are the standard deviations of three replicate measurements.

sensor offered advantages of simplicity, eco-friendliness, and large-scale production, and which made it promising for AA analysis in the food field.

Interference and selectivity of switch-on sensor

To explore the fluorescence sensing application in the food field, the interference and selectivity of the switch-on sensor were investigated. The possible coexisting metal ions (125 μmol/L), including K^+, Al^{3+}, Zn^{2+}, Mg^{2+}, Na^+, Ca^{2+}, Cu^{2+}, Fe^{2+}, Ba^{2+} and Ag^+, were also evaluated and results are shown in Fig. 5A, which showed that these metal ions had almost no quenching effects for N,S-co-CDs, and only Fe^{3+} ions could lead to obvious quenching of N,S-co-CDs, indicating that N,S-co-CDs have higher anti-interference ability for other metal ions. This phenomenon may be attributed to the specific and robust affinity between Fe^{3+} and the hydroxyl or carboxyl groups of N,S-co-CDs.

Because lots of foods contain mineral ions, organic acids, carbohydrates, and amino acids, selectivity of our developed switch-on sensor plays a vital role for AA detection in real food samples. Therefore, the selective experiment was carried out for some potentially co-existing substances, including Gly, Lys, Glu, Leu, CA, MA, TA, OA, GSH, Ca^{2+}, Na^+, and K^+. Figure 5B shows that AA exhibited the highest capability for fluorescence recovery even when the concentrations of these possible coexisting substances were much higher than that of AA. The results of Fig. 5B also suggested that Gly, Lys, Glu, Leu, OA, Ca^{2+}, Na^+ and K^+ had negligible effects on fluorescence recovery of the switch-on sensor, and TA, MA, CA and GSH have competing and reducing Fe^{3+} ability from N,S-co-CDs surface and then exhibited a weak fluorescence recovery. The interference and selectivity properties suggested that the switch-on sensor exhibited excellent selectivity for AA and could be applied for AA detection in real samples.

Application in processed fruit juice

With regard to the practical application of the developed switch-on sensor, AA content in processed fruit juice was determined. The AA content in fruit samples and the RSD compared with the reference method (HPLC) are listed in Table 1. AA content value was about 61.99, 30.91, 20.29, 9.42, and 2.81 mg/100 g for kiwi, tomato, mango, citrus reticulata, and apple, respectively, which were consistent with the China National Standards (GB 5009.86-2016) by HPLC method.

Table 1 Detection and average recovery of AA in processed fruit juice

Sample	Reference method (mg/100 g)	This work (mg/100 g)	Add amount/ μM	Average recovery, %	RSD, % (n = 3)
Kiwi	62.78	61.99	3.92	105.26	4.83
			7.84	100.05	1.48
			15.69	98.85	3.37
Tomato	28.86	30.91	4.88	99.73	3.76
			9.76	96.06	2.15
			19.51	100.31	1.97
Mango	22.81	20.29	3.28	101.79	4.45
			6.56	106.89	4.73
			13.11	95.7	2.54
Citrus reiculata	9.51	9.42	6.25	93.71	4.11
			12.5	105.19	4.37
			25	102.54	1.61
Apple	2.56	2.81	4.76	93.12	3.49
			9.52	96.21	3.13
			19.05	103.73	4.55

Additionally, the recoveries of processed fruit juice were valued using spiked method with different AA concentrations. The high recoveries ranging from 93.12 to 106.89% were obtained with favorable RSD (1.48 – 4.83%), indicating that the developed switch-on sensor exhibited potential application for selective, sensitive and accurate AA determination in processed fruit juice.

Conclusions

In summary, N,S-co-CDs were successfully synthesized by one-pot microwave-assisted method directly. N,S-co-CDs exhibited excellent fluorescence intensity, which can be quenched by Fe^{3+} and then effectively recovered in the presence of AA due to the strong reducibility of AA. Based on the phenomenon, a switch-on sensor (N,S-co-CDs/Fe^{3+}) was developed to detect AA in processed fruit juice. This sensor exhibited some appealing properties of excellent selectivity, non-interference, stability, rapid response, and high sensitivity. Notably, the sensor has been successfully applied to detect AA rapidly and sensitively in

processed fruit juice with good accuracy and precision. The most important is that such a switch-on sensor would have potential application for AA rapid determination in processed fruit juice.

Conflicts of Interest

There are no conflicts to declare.

Acknowledgements

This study was supported by the National Natural Science Foundation of China (31660482, 31701705 and 21667018), Outstanding Youth Foundation of Jiangxi (20171BCB23010), and the Open Project Program of State Key Laboratory of Food Science and Technology, Nanchang University (SKLF-KF-201813).

Supporting Information

This material is available free of charge on the Web at http://www.jsac.or.jp/analsci/.

References

1. J. N. Cobley, H. McHardy, J. P. Morton, M. G. Nikolaidis, and G. L. Close, *Free Radical Biol. Med.*, **2015**, *84*, 65.
2. R. Zhao, Y. Wang, Z. Zhang, Y. Hasebe, and D. Tao, *Anal. Sci.*, **2019**, *35*, 733.
3. H. K. Choi, X. Gao, and G. Curhan, *Arch. Intern. Med.*, **2009**, *169*, 502.
4. J. A. Drisko, J. Chapman, and V. J. Hunter, *J. Am. Coll. Nutr.*, **2003**, *22*, 118.
5. A. Pardakhty, S. Ahmadzadeh, S. Avazpour, and V. K. Gupta, *J. Mol. Liq.*, **2016**, *216*, 387.
6. T. Wu, Y. Q. Guan, and J. N. Ye, *Food Chem.*, **2007**, *100*, 1573.
7. Q. Zhu, D. Dong, X. J. Zheng, H. Q. Song, X. R. Zhao, H. L. Chen, and X. G. Chen, *RSC Adv.*, **2016**, *6*, 25047.
8. Z. Y. Yu, H. J. Li, J. H. Lu, X. M. Zhang, N. K. Liu, and X. Zhang, *Electrochim. Acta*, **2015**, *158*, 264.
9. I. Klimczak and A. Gliszczynska-Swiglo, *Food Chem.*, **2015**, *175*, 100.
10. A. Valente, A. Sanches-Silva, T. G. Albuquerque, and H. S. Costa, *Food Chem.*, **2014**, *154*, 71.
11. P. O. Barrales, M. L. F. de Cordova, and A. M. Diaz, *Anal. Chim. Acta*, **1998**, *360*, 143.
12. Z. Gazdik, O. Zitka, J. Petrlova, V. Adam, J. Zehnalek, A. Horna, V. Reznicek, M. Beklova, and R. Kizek, *Sensors*, **2008**, *8*, 7097.
13. Z. H. Liu, Q. L. Wang, L. Y. Mao, and R. X. Cai, *Anal. Chim. Acta*, **2000**, *413*, 167.
14. G. J. Kelly and E. Latzko, *J. Agric. Food Chem.*, **1980**, *28*, 1320.
15. X. Luo, W. Zhang, Y. Han, X. Chen, L. Zhu, W. Tang, J. Wang, T. Yue, and Z. Li, *Food Chem.*, **2018**, *258*, 214.
16. M. Bruchez, M. Moronne, P. Gin, S. Weiss, and A. P. Alivisatos, *Science*, **1998**, *281*, 2013.
17. L. Cui, X. P. He, and G. R. Chen, *RSC Adv.*, **2015**, *5*, 26644.
18. S. A. Nsibande and P. B. C. Forbes, *Anal. Chim. Acta*, **2016**, *945*, 9.
19. J. J. Liu, Y. L. Chen, W. F. Wang, J. Feng, M. J. Liang, S. D. Ma, and X. G. Chen, *J. Agric. Food Chem.*, **2016**, *64*, 371.
20. X. Gong, Y. Liu, Z. Yang, S. Shuang, Z. Zhang, and C. Dong, *Anal. Chim. Acta*, **2017**, *968*, 85.
21. H. B. Rao, Y. Gao, H. W. Ge, Z. Y. Zhang, X. Liu, Y. Yang, Y. Q. Liu, W. Liu, P. Zou, Y. Y. Wang, X. X. Wang, H. He, and X. Y. Zeng, *Anal. Bioanal. Chem.*, **2017**, *409*, 4517.
22. Y. L. Xu, X. Y. Niu, H. L. Chen, S. G. Zhao, and X. G. Chen, *Chin. Chem. Lett.*, **2017**, *28*, 338.
23. R. Shariati, B. Rezaei, H. R. Jamei, and A. A. Ensafi, *Anal. Sci.*, **2019**, *35*, 1083.
24. Y. H. Liu, W. X. Duan, W. Song, J. J. Liu, C. L. Ren, J. Wu, D. Liu, and H. L. Chen, *ACS Appl. Mater. Interfaces*, **2017**, *9*, 12663.
25. Q. T. Huang, H. Q. Zhang, S. R. Hu, F. M. Li, W. Weng, J. H. Chen, Q. X. Wang, Y. S. He, W. X. Zhang, and X. X. Bao, *Biosens. Bioelectron.*, **2014**, *52*, 277.
26. X. M. Li, M. C. Rui, J. Z. Song, Z. H. Shen, and H. B. Zeng, *Adv. Funct. Mater.*, **2015**, *25*, 4929.
27. A. R. Chowdhuri, T. Singh, S. K. Ghosh, and S. K. Sahu, *ACS Appl. Mater. Interfaces*, **2016**, *8*, 16573.
28. S. Singh, A. Mishra, R. Kumari, K. K. Sinha, M. K. Singh, and P. Das, *Carbon*, **2017**, *114*, 169.
29. Y. R. Park, H. Y. Jeong, Y. S. Seo, W. K. Choi, and Y. J. Hong, *Sci. Rep.*, **2017**, *7*, 46422.
30. W. Kwon, Y. H. Kim, C. L. Lee, M. Lee, H. C. Choi, T. W. Lee, and S. W. Rhee, *Nano. Lett.*, **2014**, *14*, 1306.
31. Z. S. Qian, X. Y. Shan, L. J. Chai, J. J. Ma, J. R. Chen, and H. Feng, *ACS Appl. Mater. Interfaces*, **2014**, *6*, 6797.
32. Y. J. Ju, N. Li, S. G. Liu, Y. Z. Fan, Y. Ling, N. Xiao, H. Q. Luo, and N. B. Li, *Anal. Sci.*, **2019**, *35*, 147.
33. L. B. Li, B. Yu, and T. Y. You, *Biosens. Bioelectron.*, **2015**, *74*, 263.
34. J. X. Duan, J. Yu, S. L. Feng, and L. Su, *Talanta*, **2016**, *153*, 332.
35. Y. Wang, S. H. Kim, and L. Feng, *Anal. Chim. Acta*, **2015**, *890*, 134.
36. Q. Xiao, Y. Liang, F. W. Zhu, S. Y. Lu, and S. Huang, *Microchim. Acta*, **2017**, *184*, 2429.
37. Y. Q. Zhang, X. Y. Liu, Y. Fan, X. Y. Guo, L. Zhou, Y. Lv, and J. Lin, *Nanoscale*, **2016**, *8*, 15281.
38. H. Y. Li, Y. Xu, J. Ding, L. Zhao, T. Y. Zhou, H. Ding, Y. H. Chen, and L. Ding, *Microchim. Acta*, **2018**, *185*, 276.
39. M. Shamsipur, K. Molaei, F. Molaabasi, M. Alipour, N. Alizadeh, S. Hosseinkhani, and M. Hosseini, *Talanta*, **2018**, *183*, 122.
40. M. Y. Xue, L. L. Zhang, M. B. Zou, C. Q. Lan, Z. H. Zhan, and S. L. Zhao, *Sens. Actuators, B*, **2015**, *219*, 50.
41. F. L. Zu, F. Y. Yan, Z. J. Bai, J. X. Xu, Y. Y. Wang, Y. C. Huang, and X. G. Zhou, *Microchim. Acta*, **2017**, *184*, 1899.
42. Q. Yang, J. H. Li, X. Y. Wang, H. L. Peng, H. Xiong, and L. X. Chen, *Biosens. Bioelectron.*, **2018**, *112*, 54.